Journal of Chromatography B, 908 (2012) 45–51

Contents lists available at SciVerse ScienceDirect

Journal of Chromatography B

journal homepage: www.elsevier.com/locate/chromb

Dynamic affinity chromatography in the separation of sulfated lignins binding to thrombin

Aiye Liang[a,c,d,*], Jay N. Thakkar[a,c], Michael Hindle[b], Umesh R. Desai[c,a]

[a] Department of Medicinal Chemistry, Virginia Commonwealth University, Richmond, VA, United States
[b] Department of Pharmaceutics, Virginia Commonwealth University, Richmond, VA, United States
[c] Institute for Structural Biology and Drug Discovery, Virginia Commonwealth University, Richmond, VA, United States
[d] Department of Physical Sciences, Charleston Southern University, 9200 University Boulevard, North Charleston, SC 29406, United States

ARTICLE INFO

Article history:
Received 30 July 2012
Accepted 25 September 2012
Available online 2 October 2012

Keywords:
Sulfated lignins
Heparin
Heparan sulfate
Anticoagulation
Enzyme inhibition
Dynamic affinity chromatography
Mass spectrometry

ABSTRACT

Sulfated low molecular weight lignins (LMWLs), a mixture of chemo-enzymatically prepared oligomers, have been found to be potent antagonists of coagulation. However, structures that induce anticoagulation remain unidentified. The highly polar sulfate groups on these molecules and the thousands of different structures present in these mixtures make traditional chromatographic resolution of sulfated LMWLs difficult. We performed dynamic thrombin affinity chromatography monitored using chromogenic substrate hydrolysis assay to isolate sulfated LMWL fractions that differed significantly in their biophysical and biochemical properties. Three fractions, I_{35}, I_{55} and Peak II, were isolated from the starting complex mixture. Independent plasma clotting assays suggested that I_{35} possessed good anticoagulation potential (APTT = 4.2 μM; PT = 6.8 μM), while I_{55} and Peak II were approximately 10- and 100-fold less potent. The ESI-MS spectrum of this oligomeric fraction showed multiple peaks at 684.8, 610.6, 557.4, 541.4, 536.5, and 519.4*m*/*z*, which most probably arise from variably functionalized β-*O*4—β-β-linked trimers and/or a β-*O*4—β-*O*4-linked dimers. The first direct observation of these structures in sulfated LMWLs will greatly assist in the discovery of more potent sulfated LMWL-based anticoagulants.

1. Introduction

Thrombotic disorders are a major cause of morbidity and mortality around the world. Nearly 576,000 new cases of deep vein thrombosis and pulmonary embolism, two common thrombotic conditions, are diagnosed every year in the US alone [1]. Anticoagulants are the mainstay of the treatment and prevention of these disorders. The most widely used anticoagulants include unfractionated heparin, low molecular weight heparin and warfarin. Both these anticoagulants suffer from major problems including an enhanced risk for bleeding, narrow therapeutic window, requirement for frequent monitoring, lack of oral bioavailability, hepatoxicity, thrombocytopenia and others. To address these problems, we have explored sulfated LMWLs as anionic oligomeric mimetics of polymeric heparin/heparan sulfate (Fig. 1). Sulfated LMWLs are prepared in two steps; an enzymatic coupling of 4-hydroxycinnamic acid monomers followed by chemical sulfation [2].

Sulfated LMWLs bind tightly to thrombin (and factor Xa) and inhibit coagulation [3], which is in contrast to heparins that require an intermediary co-factor antithrombin to exhibit their anticoagulant function [4]. Interestingly, the direct inhibition of thrombin by sulfated LMWLs arises from an interaction with exosite II, which reduces its enzymatic activity [3]. Such allosteric inhibition mechanism is a novel alternative to heparin's mechanism of anticoagulation and is the first instance of thrombin inhibition arising from an exclusive exosite II-mediated interaction. In addition to this unique mechanistic feature, sulfated LMWLs are structurally unique too. The oligomers possess interesting dual physicochemical properties. Sulfated LMWLs are highly hydrophilic due to their multiple anionic (sulfate and carboxylate) groups, but possess some hydrophobicity because of the presence of aromatic rings along the chains [5].

Although the novel mechanism and structure of sulfated LMWLs presents opportunities for discovery of new anticoagulants, identification of structures that cause anticoagulation has been difficult. The major challenge is the structural diversity of sulfated LMWLs, which was intentionally introduced to mimic that present in

Abbreviations: APTT, activated partial thromboplastin time assay; CE, capillary electrophoresis; DAC, dynamic affinity chromatography; ESI, electrospray ionization; FDSO3, parent sulfated lignin obtained from ferulic acid; MS, mass spectrometry; PT, prothrombin time assay; SEC, size exclusion chromatography; SDS, sodium dodecylsulfate.

* Corresponding author at: Department of Physical Sciences, Charleston Southern University, 9200 University Boulevard, North Charleston, SC 29406, United States. Tel.: +1 843 863 7833; fax: +1 843 863 7290.
E-mail addresses: aliang@csuniv.edu, liangaiye@gmail.com (A. Liang).

1570-0232/$ – see front matter © 2012 Elsevier B.V. All rights reserved.
http://dx.doi.org/10.1016/j.jchromb.2012.09.036

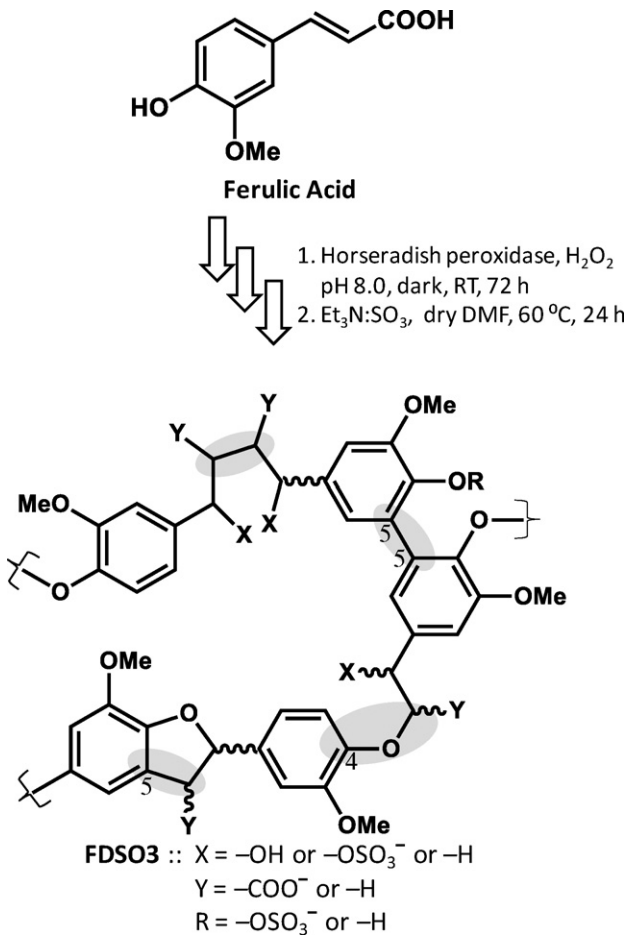

Fig. 1. Structure of FDSO3 synthesized in two steps from ferulic acid. First step was oligomerization using horseradish peroxidase (HRP) in the presence of H_2O_2 and second step was sulfation using triethylamine–sulfur trioxide complex. FDSO3 is a complex three-dimensional molecule containing β-*O*4, β-5, β-β, 5-5 inter-residue linkages (shown shaded), which are the most common linkages. Variations in X, Y, and R substituents (—H or —OSO_3^-, or —COO^-) generate large number of sequences.

polymeric heparin [2]. The oligomers are a mixture of thousands of structurally distinct chains. For example, a tetrameric sulfated LMWL chain derived from only two types of inter-residue linkages β-*O*4 and β-5 can be one of 864 theoretically possible structures. Yet, not all of these are likely to possess anticoagulant activity. Another challenge arises from the peculiar structure of sulfated LMWLs. These molecules do not bind well to reverse-phase columns. Thus, their complexity and poor binding capability result in poor separation. The molecules do interact with strong-anion exchange resins, but the high salt concentration required for elution makes MS detection difficult. Thus, the difficulty with chromatographic resolution of these molecules has also precluded structural identification.

In this work, we report on the use of dynamic affinity chromatography (DAC) to isolate and characterize sulfated LMWLs fractions. DAC monitored using chromogenic substrate hydrolysis assay led to isolation of three fractions of sulfated LMWLs, which differed significantly in their anticoagulation potential as judged by independent plasma clotting assays. Fraction I_{35} was found to the best of the three, while fraction I_{55} and Peak II were approximately 10- and 100-fold less potent. The ESI-MS spectrum of I_{35} fraction showed multiple peaks most probably arising from variably functionalized β-*O*4–β-β-linked trimers and/or a β-*O*4–β-*O*4-linked dimers. This work reports the first direct observation of these structures in sulfated LMWLs and will greatly assist in the discovery of more potent sulfated LMWL-based anticoagulants.

2. Materials and methods

2.1. Proteins, chemicals and reagents

FDSO3, a prototypic sulfated LMWL (Fig. 1), was prepared in two steps from ferulic acid, as described earlier [2,3]. Lyophilized bovine thrombin was purchased from Lee Biosolutions Inc. (St. Louis, MO). Spectrozyme TH was purchased from American Diagnostica (Greenwich, CT). Sephadex G-50, sodium dodecyl sulfate (SDS) and other chemicals were analytical reagent grade from either Sigma–Aldrich (St. Louis, MO) or Fisher Scientific (Agawam, MA). Human plasmas (citrated normal or factor VII, IX, XI, or XII-deficient) were from Haematologic Technologies (Essex Junction, VT). Deionized distilled water (ddH_2O, 18.2 MΩ), purchased from Fisher Scientific, was used as the mobile phase in the DAC. All buffers were also prepared with ddH_2O.

2.2. Dynamic affinity chromatography and thrombin inhibition monitoring

Sephadex G-50 was allowed to swell in water overnight at RT and then packed into a glass column (170 cm × 1.5 cm i.d.; total volume = 300 mL) to prepare a 150 cm long G-50 column (volume 265 mL). Bovine thrombin and FDSO3 (50 mg each) were dissolved in 3 mL high purity water and incubated for 30 min at room temperature. Following equilibration, the mixture of bovine thrombin and FDSO3 was loaded onto the Sephadex G-50 column and eluted with ddH_2O at a flow rate of approximately 0.6 mL/min. Each fraction was collected for 10 min using an ISCO Foxy 200 Fraction Collector (Cole-Parmer, Vernon Hills, IL).

For measuring the thrombin inhibition potential of each fraction from DAC, 10 μL of each fraction was diluted with 980 μL of 20 mM Tris–HCl buffer, pH 7.4, containing 100 mM NaCl, 2.5 mM $CaCl_2$, and 0.1% polyethylene glycol (PEG) 8000 in PEG 20,000-coated polystyrene cuvettes. Following this, 10 μL of 2 mM chromogenic substrate, Spectrozyme TH, was rapidly added and the residual enzyme activity was determined from the initial rate of increase in absorbance at 405 nm. The A_{405} values were plotted against fraction number to prepare the elution profile.

2.3. Quantitative measurement of thrombin inhibition potential

The IC_{50} of thrombin inhibition by FDSO3 and its fractions from DAC were measured using the chromogenic substrate hydrolysis assays, as described earlier [3]. Briefly, sulfated LMWLs (~10 μL) at varying concentrations were diluted with 20 mM Tris–HCl buffer, pH 7.4, containing 100 mM NaCl, 2.5 mM $CaCl_2$, and 0.1% polyethylene glycol (PEG) 8000 (10 μL) in PEG 20,000-coated polystyrene cuvettes, followed by addition of 5 μL of the 960 nM thrombin. Then 20 μL of 2 mM Spectrozyme TH was rapidly added and the initial rate of increase in A_{405} was measured, which correlates with the residual thrombin activity. Relative residual thrombin activity (Y) at each concentration of FDSO3 or its derivatives was calculated from the ratio of residual thrombin activity in the presence of the inhibitors to that in their absence. Logistic Eq. (1) was used to fit the dose dependence of residual thrombin activity to derive the IC_{50} and HS. In this equation, Y_M and Y_O are the maximum and minimum values of the fractional residual thrombin activity, and IC_{50} is the concentration of the inhibitor that results in 50% inhibition of enzyme activity. Sigmaplot 8.0 (SPSS Inc., Chicago, IL) was

used to perform nonlinear curve fitting in which Y_M, Y_O, and IC_{50} were allowed to float.

$$Y = Y_O + \frac{Y_M - Y_O}{1 + 10^{(\log [FDSO3]_0 - \log IC_{50})}} \quad (1)$$

2.4. Plasma clotting assays

Human plasma clotting time was determined in a standard 1-stage recalcification assay with a BBL Fibrosystem fibrometer (Becton-Dickinson, Sparles, MD). For prothrombin time (PT), 10 μL FDSO3 (or its chromatographic fractions) was mixed with 90 μL of citrated normal human plasma or factor VII, IX, XI, or XII deficient human plasma, incubated for 30 s at 37 °C followed by addition of 200 μL pre-warmed thromboplastin. For activated partial thromboplastin time (APTT), 10 μL FDSO3 (or its fractions) was mixed with 90 μL of citrated normal human plasma or factor VII, IX, XI, or XII deficient human plasma and 100 μL of 0.2% ellagic acid, incubated for 240 s at 37 °C followed by addition of 100 μL of 25 mM $CaCl_2$. Each experiment was performed at least twice. The averaged data was used to calculate the concentration of the anticoagulant necessary to increase the clotting time by 50% (1.5 × APTT or 1.5 × PT).

2.5. Capillary electrophoretic characterization of FDSO3 and its fractions

Capillary electrophoresis (CE) experiments were performed using a Beckman P/ACE MDQ system (Fullerton, CA). Electrophoresis was performed at 25 °C in a constant voltage mode (8 kV) using an uncoated fused silica capillary (75 μm) with the total and effective lengths of 31.2 cm and 21 cm, respectively. The detection wavelength was set at 214 nm. A sequential wash of 1 M HCl (10 min), water (5 min), 1 M NaOH (10 min), and water (5 min) at 20 psi was used to activate a capillary. Before each electrophoretic run, the capillary was rinsed with the running buffer for 3 min at 20 psi. In normal polarity, the samples were injected at the anode and detected at the cathode. The buffers used in normal polarity experiments included 20 mM Tris–HCl, pH 8.5, or 20 mM sodium phosphate, either pH 7.4 or 8.0. For reverse polarity experiments, the sample was injected at the cathode (0.5 psi for 5 s, or 1 psi for 10 s) and detected at the anode. The buffer used in reverse polarity experiments was 50 mM sodium phosphate, pH 3.0.

2.6. Size exclusion chromatographic characterization of FDSO3 and its fractions

The average molecular weights of FDSO3 and its fractions were determined using a Shodex Asahipak GS-320 HQ size-exclusion (SEC) column (Showa Denko America Inc., New York, NY) and Shimadzu Class VP HPLC connected to a UV–vis detector (Shimadzu Scientific Instruments, Columbia, MD). FDSO3 (10 μL), or its fractions, were eluted with 0.1 M NaOH at 0.7 mL/min and detected at 280 nm. Polystyrene sulfonates (PSS) of molecular weights 4200–33,000 from American Polymer Standards (Mentor, OH) were used as standards. The average molecular weights (M_R) of FDSO3 and its fractions were calculated from the linear calibration curve ($\log M_R = m \times V_E + c$; V_E is the volume of elution; m and c are constants) prepared with PSS standards.

2.7. Mass spectrometric characterization of FDSO3 and its fractions

Mass spectrometry was performed on FDSO3 and its fractions using a Micromass ZMD4000 single quadrupole mass spectrometer with ESI ionization probe operating in both negative and positive ion modes (Waters Corp., Milford, MA). Stock samples were prepared in ddH_2O at 300–320 μM concentration. For negative mode, the stock solutions were further diluted in acetonitrile-containing 20% formic acid (5%, v/v) to give 1–10 μM solutions and infused at 10 μL/min and optimal ionization conditions were deduced in real time. The source block temperature and the capillary probe temperature were held at 100 and 120 °C, respectively. Capillary and cone voltages of 3.32 kV and 38 V were selected following optimization. The nitrogen flow for desolvation was 50 L/h. Mass spectra were acquired in the mass range from 100 to 1800 Da at 400 amu/s. For the positive mode, the samples were dissolved in acetonitrile-containing 20% formic acid (5%, v/v). The source block temperature and the capillary probe temperature were held at 150 and 120 °C, respectively. Capillary and cone voltages of 3.85 kV and 38 V were selected following optimization. Mass spectra were acquired in the mass range from 450 to 700 Da at 400 amu/s with an accuracy of ±1 amu. All the other conditions were same as the negative mode.

3. Results

3.1. Development of dynamic affinity chromatography (DAC) for fractionation of FDSO3

FDSO3, a sulfated LMWL, has been found to directly inhibit thrombin with IC_{50} of 0.03 μM [3]. FDSO3 is a heterogeneous oligomer comprised of a number of chains with distinct structures. We hypothesized that select group of chains in FDSO3 may inhibit thrombin (and other coagulation enzymes). To identify such chains, we first attempted resolving FDSO3 into high and low affinity fractions using traditional affinity chromatographic separation. Thrombin affinity columns were prepared using *N*-hydroxysuccinimide-activated Hi-Trap columns. However, elution with salt gradient (0 → 3 M) did not release any (neither high- nor low/no-affinity) FDSO3 from the column. Investigation of the problem showed that the Hi-Trap matrix did not release FDSO3 possibly because of the highly cross-linked hydrophobic matrix. Elution with aqueous solutions did not release FDSO3, but alcohol-based eluents led to partial release of the oligomer. Other affinity or anion exchange matrices including NHS-activated Sepharose 4 fast flow, ω-aminohexyl-Agarose, ω-aminohexyl-Sepharose 4B and diethylaminoethyl-cellulose also retained more than 90% FDSO3.

In contrast, Sephadex G-15, G-25 or G-50 matrices did not retain much FDSO3 suggesting the possibility of using DAC for fractionation purposes. Thus, a pre-formed complex of thrombin and FDSO3 was loaded on a Sephadex G-50 sizing column and then slowly eluted at pH 7.0. The equilibrium between thrombin and FDSO3 is a dynamic process, which eventually retains FDSO3 molecules that possess higher affinity for thrombin, resulting in resolution of high and low/no affinity fractions. The resolution of FDSO3 was monitored through absorbance at 280 nm, which detects both FDSO3 and thrombin, as well as through Spectrozyme TH hydrolysis assay, which quantifies the level of thrombin activity. Fig. 2A shows a representative elution profile. The A280 profile showed that the FDSO3 mixture separated into two major peaks, labeled Peaks I and II. FDSO3 has a characteristic yellow color, which was vividly present in both peaks. Control experiments with thrombin and FDSO3 alone revealed that the enzyme is present in the earlier fractions, while the sulfated LMWL elutes as a wide peak stretching from fractions 18 to 60 (Fig. 2B). Thus, Peak I was hypothesized to be thrombin – higher affinity FDSO3 complex, while Peak II thought to be low/no affinity FDSO3.

To investigate whether this expectation was correct, thrombin activity of each fraction was measured using chromogenic substrate hydrolysis assay under pseudo-first order conditions. The initial linear increase in A_{405}, which corresponds directly to

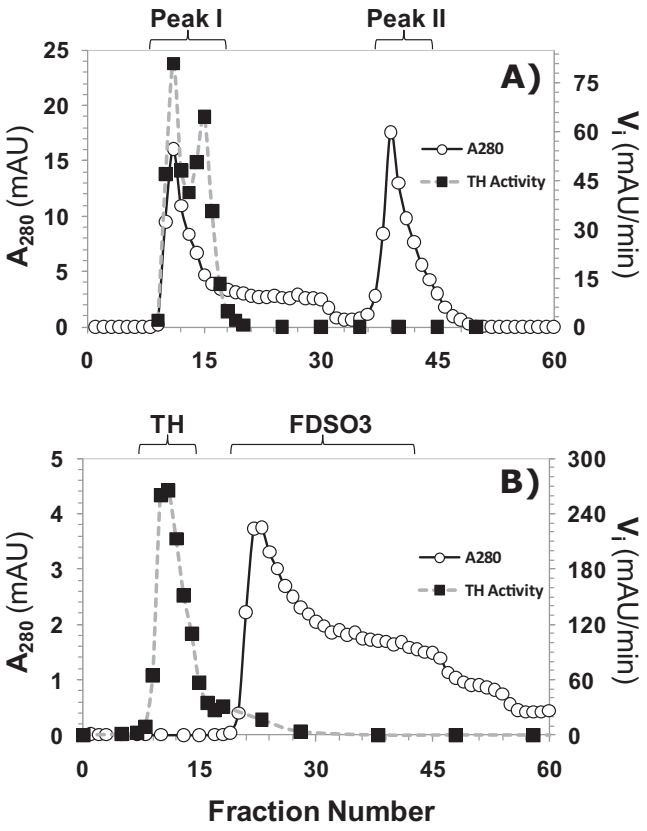

Fig. 2. Thrombin DAC to isolate FDSO3 fraction that binds thrombin with higher affinity. (A) FDSO3 and bovine thrombin (1:1 mass ratio) were loaded on a Sephadex G-50 column and then eluted with water to collect 60–80 fractions of 4–7 mL each. The elution profile was followed spectrophotometrically (A_{280} values on the *y*-axis on the left, -○-) as well as by measuring thrombin activity (initial rate of substrate hydrolysis on the *y*-axis on the right, -■-). Fractions 7–18 and 35–52 were pooled as Peaks I and II, respectively. (B) Two control experiments in which FDSO3 and thrombin were loaded separately on the same Sephadex G-50 column under otherwise identical conditions.

thrombin activity, was found to reach values of 60–75 mAU/min for fractions corresponding to Peak I, while Peak II fractions displayed complete absence of thrombin's hydrolytic activity. Control experiments showed that fractions from the thrombin alone column gave slopes of ~270 mAU/min (Fig. 2B), which confirmed that Peak I of the dynamic affinity column contained thrombin as well as FDSO3.

3.2. Isolation of thrombin–free FDSO3 species from Peak I

To isolate FDSO3 free from thrombin, we incubated thrombin–FDSO3 complex with SDS, a denaturant that could release the hydrophobic ligand. We found that 0.01% (w/v) SDS was the least concentration of the denaturant that could release FDSO3, as detected by capillary electrophoresis (not shown). Hence, peak I fractions from the DAC were pooled, lyophilized, dissolved in 0.01% SDS at room temperature and re-chromatographed on Sephadex G-50. Fractions collected from this SEC were analyzed in a manner similar to that from the DAC runs. Three peaks were detected using absorbance at 280 nm (Fig. 3). The first peak displayed thrombin activity, while also showing all the characteristics of FDSO3. This suggested that part of FDSO3, may be of higher affinity, was still bound to thrombin. The second and third peaks, labeled as Peaks I_{35} and I_{55}, respectively, displayed the characteristic yellow color, but no thrombin activity (see Fig. 3). This indicated that I_{35} and I_{55} are FDSO3 chains released from

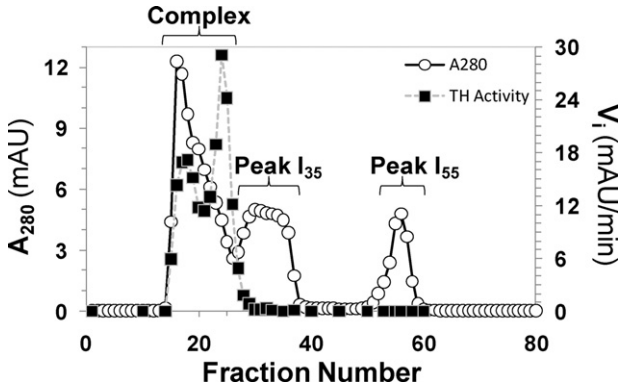

Fig. 3. DAC in 0.01%SDS to release FDSO3 chains bound to thrombin. The FDSO3–bovine thrombin complex isolated from the first dynamic affinity column (see Fig. 2) was incubated with 0.01% SDS and fractionated on Sephadex G-50. The elution profile was followed spectrophotometrically (A_{280}, -○-) as well as by measuring thrombin activity (-■-). Two fractions were isolated – Peak I_{35} (fractions 34–40) and Peak I_{55} (fractions 55–60).

thrombin upon 0.01% SDS treatment. CE analysis of I_{35} and I_{55} under reverse polarity conditions displayed bands at about 8 min in a manner similar to FDSO3 supporting the conclusion that I_{35} and I_{55} are FDSO3 species free of thrombin (not shown).

3.3. Average molecular weight of FDSO3 and its fractions

Although isolated from thrombin through DAC, I_{35} and I_{55} were still expected to be heterogeneous mixtures. Thus, we measured the average molecular weights of these fractions, as previously described using high performance SEC [2]. Polystyrene sulfonate standards were used to prepare a calibration curve (not shown). Using this calibration, the number, weight and peak average molecular weights (M_N, M_W and M_P) of FDSO3, I_{35}, I_{55} and Peak II were obtained (Table 1). The average molecular weight of FDSO3 prepared for study was found to be slightly higher than those reported earlier [2] suggesting small variations in the free radical-driven oligomerization reaction. The M_P values of the four samples were found to be 6490, 6650, 2910, and 1930 (Table 1) with a polydispersity of 1.7, 1.8, 2.2 and 4.5, respectively. These results suggest that on average I_{55} and Peak II are significantly different from FDSO3 and I_{35}. More importantly, the results imply that despite fractionation I_{35} was rather similar to the parent FDSO3 in overall size of the chains. Using the molecular weight of the monomer, the average chain length of FDSO3 and I_{35} was calculated to be 33 and 34 units, respectively. This indicates a considerably long polymeric chain for both FDSO3 and I_{35}. In contrast, I_{55} and Peak II were found to be considerably shorter on average.

3.4. In vitro anticoagulant potential of FDSO3 and its fractions in normal human plasma

To assess plasma anticoagulant potential of I_{35} and I_{55}, we measured prothrombin and activated partial thromboplastin times (PT and APTT). Clotting assays are typically used to assess coagulation state of plasma. The coagulation cascade is traditionally divided into intrinsic and extrinsic pathways, which are comprised of distinct coagulation factors, although it is well established that both pathways are highly intertwined with multiple feedback and feed-forward loops [6]. Traditionally, PT measures the state of extrinsic pathway, which is primarily comprised of factor VII and tissue factor; while APTT relates more with the intrinsic pathway, which includes factors IX, XI and XII. In addition, PT and APTT also depend on the state of factors II and X, which belong to the common pathway.

Table 1
Biophysical and biochemical properties of FDSO3 and its affinity fractions.

	M_N [a] (Da)	M_W [a] (Da)	M_P [a] (Da)	P[b]	L_R [c]	IC_{50} [d] (μg/mL)	IC_{50} [d] (μM)	Y_0 [d]	Y_M [d]
FDSO3	4810	8230	6490	1.71	~33	0.97 ± 0.13[e,f]	0.15 ± 0.02	0.26 ± 0.01	1.01 ± 0.01
I_{35}	4250	7690	6650	1.81	~34	319 ± 51	47.9 ± 7.7	0.23 ± 0.05	0.92 ± 0.04
I_{55}	2120	4600	2910	2.17	~15	103 ± 22	35.5 ± 7.4	0.24 ± 0.12	1.02 ± 0.01
Peak II	440	1960	1930	4.45	~10	141 ± 20	73.1 ± 10.1	0.30 ± 0.05	0.98 ± 0.03

[a] Number, weight and peak average molecular weights were obtained by SEC analysis.
[b] Polydispersity.
[c] The peak average chain length was calculated from the ratio of M_P and molecular weight of the monomer, ferulic acid.
[d] Parameters IC_{50}, Y_M, and Y_0 are defined in Section 2 and were obtained from nonlinear regression analysis of direct inhibition of thrombin at pH 7.4 and 25 °C.
[e] IC_{50} calculation uses M_P values.
[f] Errors represent ±1SE.

Clotting times were measured with citrated human plasma at six to eight concentrations of parent FDSO3, I_{35}, I_{55} and Peak II. The clotting times increased with the concentration of each sample under either APTT or PT conditions (see Supplementary Figure S1) and the profile could be fitted using a quadratic equation, which was used to calculate the concentration of the anticoagulant necessary to increase the clotting time by 50% (represented as 1.5 × APTT). FDSO3, I_{35}, I_{55} and Peak II displayed 1.5 × APTT values of 3.3, 4.2, 63 and >500 μM, respectively, indicating that I_{55} and Peak II were indeed much less anticoagulant in plasma, as expected on the basis of in vitro thrombin inhibition potential. These fractions were therefore not investigated further. In PT assays, FDSO3 and I_{35} displayed 1.5 × PT values of 5.9 and 6.8 μM, respectively (Table 2).

To assess whether the different fractions exhibit varying thrombin inhibition potential, we performed Spectrozyme TH hydrolysis in the presence of I_{35}, I_{55} and Peak II, as previously described [3]. As the concentration of the potential anticoagulant was increased, the residual thrombin activity progressively decreased (see Supplementary Figure S2), which could be fitted by the logistic dose–response Eq. (1) to derive IC_{50} and HS (Table 1). The IC_{50} was found to be 48, 36, and 73 μM for I_{35}, I_{55} and Peak II, respectively. The results show that there is marginal difference in inhibition potential of the three affinity-resolved fractions. This implies that resolution achieved through DAC does not automatically result in high thrombin inhibition potential for this group of molecules.

Table 2
APTT and PT values measured for FDSO3 and its fractions in normal and factor VII, IX, XI or XII-deficient human plasma.

Fractions	Plasma	Time to clot[a]	
		(μg/mL)	(μM)
Activated partial thromboplastin time			
FDSO3	Normal	21.5	3.31
FDSO3	fIX-deficient	47.3	7.29
FDSO3	fXI-deficient	27.7	4.27
FDSO3	fXII-deficient	51.4	7.92
I_{35}	Normal	28.0	4.2
I_{35}	fIX-deficient	65.0	9.8
I_{35}	fXI-deficient	12.0	1.8
I_{35}	fXII-deficient	79.0	11.9
I_{55}	Normal	183	63
Peak II	Normal	>1000	>500
Prothrombin time			
FDSO3	Normal	38.5	5.9
FDSO3	fVII-deficient	69.3	10.7
I_{35}	Normal	45.5	6.8
I_{35}	fVII-deficient	No effect	No effect

[a] Clotting time was determined in a standard 1-stage re-calcification assay as described in Section 2. Experiments were performed at least twice and averaged to calculate the concentration of the anticoagulant necessary to increase the time to clot by 50% (1.5 × APTT or 1.5 × PT).

3.5. Anticoagulant potential of I_{35} in coagulation factor deficient human plasma

Fraction I_{35} exhibits strong plasma anticoagulation although its ability to inhibit thrombin is not high. An explanation is that I_{35} is a specialized fraction of FDSO3 that targets other coagulation enzyme(s) better than thrombin. To test this hypothesis, plasma clotting assays were performed using coagulation factor-deficient human plasma. The hypothesis is that if I_{35} inhibits one or more extrinsic pathway or intrinsic pathway factors, deficiency of that coagulation factor will induce dysfunction in anticoagulation.

To test this hypothesis, APTT assays were performed with factor IX, XI or XII-deficient human plasmas (see Supplementary Figure S3B). The 1.5 × APTT was found to be 7.3, 4.3 and 7.9 μM for FDSO3 (Table 2), while I_{35} displayed values of 9.8, 1.8 and 11.9 μM for factor IX, XI and XII-deficient plasma, respectively. This indicates that I_{35} was almost equal in anticoagulant activity as FDSO3. Thus, I_{35} does not appear to inhibit an intrinsic factor to exhibit its anticoagulant effect.

When the experiment was performed with factor VII-deficient human plasma, the clotting time increased as a function of FDSO3 dose, but was unaffected by the presence of I_{35}. In fact, the 1.5 × PT value for FDSO3 was found to be 10.7 μM, while that for I_{35} could not be measured with confidence (Table 2, see Supplementary Figure S3A). This indicates that the absence of factor VII introduced a major defect in the anticoagulant activity of I_{35}, while FDSO3 continues to essentially fully functional. The result indicates that fraction I_{35} obtained from DAC is likely to inhibit proteins of the extrinsic pathway, which include factor VII, factor VIIa, tissue factor, or their complex.

3.6. Mass spectrometric characterization of I_{35}

Mass spectrometry (MS) is a particular useful technique for structural characterization of highly charged molecules [2,7–9]. Sulfated LMWLs present major problems because of their massive heterogeneity and polydispersity. While MS of heparin and heparan sulfates has succeeded to a reasonable extent [7–9], sulfated lignins with high molecular weights have not yielded much success. The primary reason for this is the instability of the polyphenolic structure even under mild ionization conditions, such as ESI [10–12]. A secondary reason is that anionic higher molecular weight species are difficult to volatilize. Nevertheless, we explored the applicability of ESI-MS to characterize I_{35}. Specifically, a key question to address was whether selected inter-monomeric linkages, of the many possible for FDSO3, are enriched in I_{35}.

The ESI-MS spectrum of I_{35} in the positive ion mode (Fig. 4A) displayed a group of peaks with good intensity. Ten peaks p1–p10 were observed in the range of 400–700m/z, each corresponding to a singly charged ion. To pinpoint the plausible structures of the LMWL species, a library of all possible dimers, trimers and

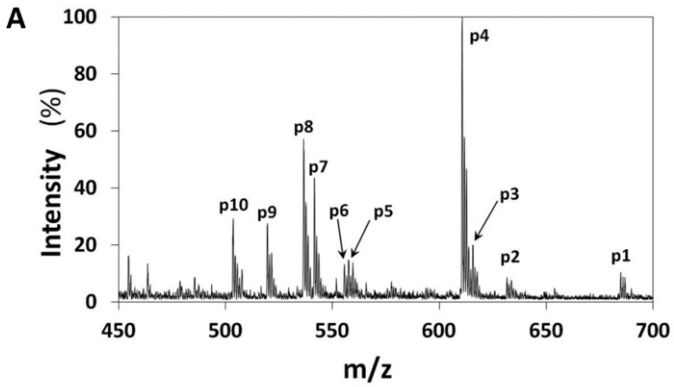

	Substituents										[M+Na]⁺ (m/z)	
	R	X_1	X_2	X_3	Y_1	Y_2	Y_3	b_1	b_2	b_3	Obsd	Calc
p1	-SO_3H	-H	-H	-H	-COOH	-COOH	-COOH	d	s	s	684.77	685.13
p2	-SO_3H	-OH	-OH	-OH	-COOH	-H	-H	s	s	s	631.45	631.15
p3	-SO_3H	-H	-H	-H	-COOH	-COOH	-H	d	d	d	615.49	615.11*
p4	-SO_3H	-OH	-H	-H	-COOH	-H	-H	s	d	d	610.64	611.12
p5	-H	-H	-H	-H	-COOH	-COOH	-H	d	d	d	557.38	557.14
p6	-SO_3H	-H	-H	-H	-H	-H	-H	s	s	s	555.42	555.17
p7	-H	-H	-H	-H	-COOH	-COOH	-H	s	s	s	541.43	541.20*
p8	-H	-H	-H	-H	-COOH	-COOH	-H	d	d	s	536.46	537.17*
p9	-H	-H	-H	-H	-COOH	-H	-H	s	s	s	519.39	519.20
p10	-SO3H	-OH	-OH	na	-COOH	-COOH	na	s	d	na	503.44	503.08*

Fig. 4. ESI-MS of I_{35}. Fraction I_{35} was directly infused in the mass spectrometer while scanning in the mass range 400–700*m*/*z* units in positive-ion mode with a mass accuracy of ±1 amu. Peaks p1–p10 were observed in a reproducible manner (A). Each peak is a monocharged ion and can be assigned to variably substituted β-*O*4—β-β-linked FDSO3 trimers, except for p10, which corresponds to a dimer (B). Variable substitution in trimers arises from R, X_1, X_2, X_3, Y_1, Y_2, and Y_3 substituents (shown in shaded ovals in part A) or from the variation in bond type (b_1, b_2 and b_3), which can be either a single (s) or a double bond (d). Asterisk (*) indicates peaks best analyzed as $[M+H]^+$. Remaining peaks were best found to fit $[M+Na]^+$ species. 'na' refers to not-applicable. See text for details.

tetramers was generated using standard structure building tools. Substituents, such as —H, —OH, —OSO_3H, and —COOH as well as single or double bond at appropriate positions in the inter-monomeric linkages, as dictated by the free-radical mechanism of enzymatic oligomerization [13], were considered in generating this library. This combinatorial library was found to contain nearly 5000 cationic species (either H^+ or Na^+ forms). Comparison of the observed *m*/*z* values with those calculated for dimers, trimers and tetramers led to the identification of a small group of LMWL structures that satisfy the ESI-MS profile of I_{35} (Fig. 4B).

Nine of the ten peaks, i.e., p1–p9, could be explained on the basis of a β-*O*4—β-β trimeric structure, whereas a β*O*4—β*O*4 dimer was found to match the p10*m*/*z*. Five trimers and the dimer contained a sulfate moiety (—OSO_3H) suggesting the importance of this group. Also, peaks p2, p9 and p10 contained one; peaks p1, p3, p5, p7 and p8 contained two, and peak p1 contained three —COOH group(s). This makes carboxylic acid moiety the most common group present in the species observed. Other smaller differences include the presence of a hydroxyl group at the benzylic position of the monomers (X substituent) and the presence of a double bond on the inter-residue linkage. These variations arise from the quenching and/or subsequent dehydration of a benzylic free radical during synthesis. Overall, the results suggest that the group of molecules identified are derived from the parent sulfated or unsulfated trimers and represent a relatively small group of closely related structures.

It is important to recognize that although the structures shown in Fig. 4B can explain the ten peaks observed in the ESI-MS spectrum of I_{35}, the number of distinct structural possibilities that fit the structures are many more. For example, the —OSO_3H group can be placed also on the other end of trimer, which is chemically indistinguishable in this analysis. Likewise, most variations shown, i.e., X, Y, and b (see Fig. 4B), can display other degenerate possibilities. Further, the presence of two chiral centers per monomer suggests that the number of distinct structures that can explain peaks p1–p10 of Fig. 4B are much greater than that presented in this simplified analysis.

4. Discussion

This work began with a rather simple goal of deducing structure of sulfated LMWLs that preferentially recognize coagulation enzymes so as to aid the discovery of potentially new molecules as anticoagulants that work through an allosteric mechanism. An overwhelming number of orthosteric inhibitors of thrombin and factor Xa have been designed [6,14,15] and our discovery that sulfated LMWLs utilized a radically different mechanism [3] suggested a strong possibility of uncovering potent oligomeric allosteric anticoagulants.

However, the major challenge to uncovering distinct molecules based on sulfated LMWLs is the complexity of the lignin scaffold. Natural lignins are biosynthesized through the action of peroxidases on 4-hydroxy cinnamyl alcohols to give polymers containing multiple inter-residue linkages, of which the most common include β-*O*4, β-5, β-β and 5-5 [13]. Chemo-enzymatically prepared LMWLs, especially the sulfated LMWLs studied here, may contain additional variations because of the presence or absence of sulfate (—OSO_3^-), carboxylate (—COO^-) and hydroxyl (—OH) substituents. Further, the free radical mechanism of oligomerization gives all possible stereoisomers [16]. These combinations result in a large number of sequences. In fact, 10^{66} different primary, natural lignin structures have been proposed by some authors [17], although this may not necessarily be true for our chemo-enzymatically prepared sulfated LMWLs.

Another problem discovered with sulfated LMWLs was their combination of hydrophilicity and hydrophobicity in addition to three-dimensional macromolecular structure. Strong hydrophilicity arises from the many sulfates and carboxylates on the lignin scaffold, while hydrophobicity arises from its aromatic groups. This implies that traditional reverse-phase based separation does not work because the molecules do not stick to C-18 columns, while the aromatic macromolecular scaffold is possibly the main reason why these oligomers get entangled in affinity matrices. We resolved the problem of matrices in covalent thrombin columns by using a dynamic affinity column. The successful collection of FDSO3–thrombin complex following a dynamic equilibrium affinity column indicates that the complex has low dissociation constant. However, treatment with the mildest form of the denaturant (0.01% SDS) appears to have preferentially released FDSO3 forms, i.e., I_{35} and I_{55}, that are not potent inhibitors of thrombin. This implies that FDSO3 chains with higher thrombin affinity remained bound to thrombin even after treatment with 0.01% SDS. This also implies that FDSO3 fractions with better thrombin inhibition potential could be possibly released with higher levels of the denaturant in DAC.

The observation that I_{35} is essentially ineffective in factor VII-deficient plasma, while being nearly fully functional in other coagulation factor-deficient plasmas indicates that certain chains of FDSO3 possess specificity for proteins of the extrinsic pathway. This is an interesting observation and indicates that certain FDSO3 species appear to possess structural recognition elements for distinct proteins of the coagulation cascade. The observation does not directly implicate factor VIIa because tissue factor is also a

key protein involved in this process, which implies I_{35} may target either factor VII, factor VIIa or tissue factor. However, the experiments highlight the value of DAC in identification of novel activities present in FDSO3.

To identify structural features of I_{35}, we resorted to ESI-MS, which is a highly sensitive method applicable on small amounts of material isolated with difficulty. Also, the heterogeneity and complexity of I_{35} makes standard techniques, e.g., NMR, not particularly useful for elucidation of fine structure [18]. MS of lignins has typically provided key information of smaller lignin chains. Longer lignin chains have been found to be susceptible to widespread fragmentation even under mild ionization conditions of ESI. The ESI-MS spectrum of I_{35} displayed 10 peaks, which most probably represent chains present in significant quantities and therefore are characteristic of the structural composition. We assumed that only four common inter-residue linkages (β-*O*4, β-5, 5-5 and β-β) are present in the sulfated LMWL being studied. The observed ESI-MS profile was analyzed as a composite of nine β-*O*4–β-β trimers and one β-*O*4–β-*O*4 dimer. This implies that I_{35} is considerably enriched in β-*O*4–β-β-linked oligomers suggesting that this unit is likely to be important for targeting the extrinsic pathway. This is the first direct evidence of sulfated LMWL structures that antagonize human plasma clotting.

Yet, a word of caution is in order. The determination of exact structures of these molecules will require additional information including NMR/X-ray data and unambiguous synthesis. Unfortunately, NMR requires significant quantities of material, while X-ray requires crystals. Both are difficult because of the nature of sulfated lignins. The amounts separated by dynamic affinity chromatography are small at the present. The fraction analyzed by ESI-MS is still a mixture of several molecules, which makes crystallography challenging. Added to these difficulties is the significant structural degeneracy of sulfated LMWLs. Advanced MS techniques including tandem MS using collision induced fragmentation may help identify precise structures. Finally, a foolproof way to identify potent inhibitors is to undertake chemical synthesis of a small library of suggested oligomers.

Despite these difficulties, overall DAC has provided the first glimpse on the possible structures that may be responsible for the powerful anticoagulant activity of sulfated lignins. Interestingly, a fraction that inhibits coagulation through the extrinsic pathway was identified. This is first direct observation of distinct structures of sulfated lignins and will greatly assist in the discovery of more potent sulfated LMWL-based anticoagulants.

Acknowledgements

This work was supported by grants HL099420 and HL090586 from the National Institutes of Health, grant EIA 0640053N from the American Heart Association National Center, and grant 6-46064 from the A. D. Williams Foundation.

Appendix A. Supplementary data

Supplementary data associated with this article can be found, in the online version, at http://dx.doi.org/10.1016/j.jchromb.2012.09.036.

References

[1] M. Cushman, A.W. Tsai, R.H. White, S.R. Heckbert, W.D. Rosamond, P. Enright, A.R. Folsom, Am. J. Med. 117 (2004) 19.
[2] B.H. Monien, B.L. Henry, A. Raghuraman, M. Hindle, U.R. Desai, Bioorg. Med. Chem. 14 (2006) 7988.
[3] B.L. Henry, B.H. Monien, P.E. Bock, U.R. Desai, J. Biol. Chem. 282 (2007) 31891.
[4] U.R. Desai, Med. Res. Rev. 24 (2004) 151.
[5] A. Liang, J.N. Thakkar, U.R. Desai, J. Pharm. Sci. 99 (2010) 1207.
[6] B.L. Henry, U.R. Desai, Cardiovasc. Haematol. Agents Med. Chem. 6 (2008) 323.
[7] M.M. Siegel, K. Tabei, M.Z. Kagan, I.R. Vlahov, R.E. Hileman, R.J.J. Linhardt, Mass Spectrom. 32 (1997) 760.
[8] W. Chai, J. Luo, C.K. Lim, A.M. Lawson, Anal. Chem. 70 (1998) 2060.
[9] B. Kuberan, M. Lech, L. Zhang, Z.L. Wu, D.L. Beeler, R.D. Rosenberg, J. Am. Chem. Soc. 124 (2002) 8708.
[10] S. Reale, A. Di Tullio, N. Spreti, F. De Angelis, Mass Spectrom. Rev. 23 (2004) 87.
[11] D.V. Evtuguin, P. Domingues, F.L. Amado, C.P. Neto, A.J.F. Correia, Holzforschung 53 (1999) 525.
[12] J.H. Banoub, B. Benjelloun-Mlayah, F. Ziarelli, N. Joly, M. Delmas, Rapid Commun. Mass Spectrom. 21 (2007) 2867.
[13] W. Boerjan, J. Ralph, M. Baucher, Annu. Rev. Plant Biol. 54 (2003) 519.
[14] B.L. Henry, U.R. Desai, in: D.J. Abraham, D.P. Rotella (Eds.), Burger's Medicinal Chemistry, Drug Discovery and Development, seventh ed., John Wiley, Hoboken, 2010, p. 365.
[15] A. Straub, S. Roehrig, A. Hillisch, Angew. Chem. Int. Ed. 50 (2011) 4574.
[16] J. Ralph, J. Peng, F. Lu, R.D. Hatfield, R.F. Helm, J. Agric. Food Chem. 47 (1999) 2991.
[17] J. Ralph, K. Lundquist, G. Brunow, F. Lu, H. Kim, P.F. Schatz, J.M. Marita, R.D. Hatfield, J.H. Christensen, W. Boerjan, Phytochem. Rev. 3 (2004) 29.
[18] J.M. Marita, J. Ralph, R.D. Hatfield, C. Chapple, Proc. Natl. Acad. Sci. U.S.A. 96 (1999) 12328.